Modelling and control of a wind turbine equipped with a permanent magnet synchronous generator (PMSG)

J. Salazar[(a)], F. Tadeo[(b)], C. de Prada[(c)], L. Palacin[(d)]

[(a) (b) (c)]Dpt of System Engineering and automatic control, Faculty of Science, University of Valladolid, Spain
[(d)] Sugar Technology Center (CTA), Valladolid, Spain

[(a)] johanna@autom.uva.es, [(b)] fernando@autom.uva.es, [(c)] prada@autom.uva.es, [(d)] palacin@cta.uva.es

ABSTRACT
This paper describes the dynamic models for a wind turbine system equipped with a permanent magnet synchronous generator (PMSG) and a back-to-back Voltage Source Converter, which is operated with the Space Vector Modulation Technique using a symmetric switching sequence. The generator side converter works as a three-phase rectifier and the grid side converter works as an inverter, which is used to interface the wind turbine system with the stand-alone hybrid system. All the components of the wind turbine system, including a typical generator side controller and except the DC-link and the grid side converter were analyzed. These dynamic models can be used for dynamic simulation in order to test different configurations, as well as control strategies and fault detection and accommodation algorithms.

Keywords - wind turbines, pitch angle control, Permanent magnet generator, three-phase PWM rectifiers, Space Vector Modulation, Symmetric Switching Sequence.

I. INTRODUCTION

The objective of this paper is to develop computer models for a variable speed Wind Turbine System (WTS) equipped with PMSG that can be used for dynamic simulation to test different configurations, as well as control strategies and fault detection and accommodation algorithms.
One of the problems associated with variable-speed wind turbine systems is the presence of the gearbox coupling the wind turbine to the generator. This mechanical element suffers from considerable faults and increases maintenance expenses. In order to improve reliability of the wind turbine and reduce maintenance expenses, the gearbox is frequently eliminated. Hence, a variable speed wind turbines equipped with Permanent Magnet Synchronous Generators (PSMG) and power converters are being used more frequently in wind turbine application [1,2].
The conventional power converter for a small power wind turbine system (WTS) is shown in Fig. 1, which consists of the diode rectifier, boost circuit, and a grid side converter[3]. Since the uncontrolled diode rectifier is connected to the PMSG, it is not possible to control the generator speed for output power control. Moreover, high harmonic distortion currents are obtained in the generator that might reduce efficiency and produce torque oscillations.

Figure 2 shows the scheme for a variable speed wind turbine system based on a permanent magnet synchronous generator, which is analyzed in this paper. This wind turbine system is connected to the AC side of a stand-alone hybrid system which includes a battery storage system, a diesel generator and a photovoltaic system as a renewable source. This hybrid system combines with a reverse osmosis desalinization unit will be used to supply fresh water and electricity to rural remote communities not connected to the public grid. The whole designed plant is installed in the site of Bordj Cedria in Tunisia in CRTEn (Centre de Recherche et des Technologies de l'Enegie) [4].
This wind turbine system consists of a Permanent Magnet Synchronous Generator (PMSG) connected to a power electronic system, which is composed of a back-to-back Voltage Source Converter (VSC), where the generator side converter works as a three-phase rectifier and the grid side converter works as an inverter [5] This paper is focused mainly on the generator side, only the wind turbine components and generator side controller until the DC-link.

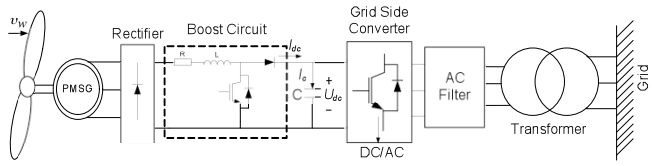

Figure 1.- Conventional block diagram of a wind turbine with PMSG

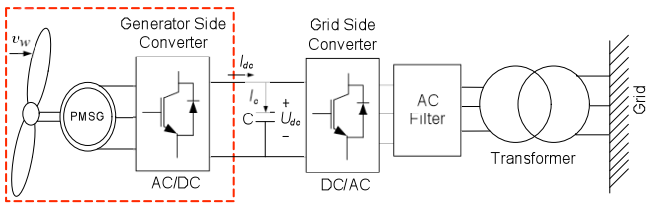

Figure 2.- Block diagram of a wind turbine with PMSG

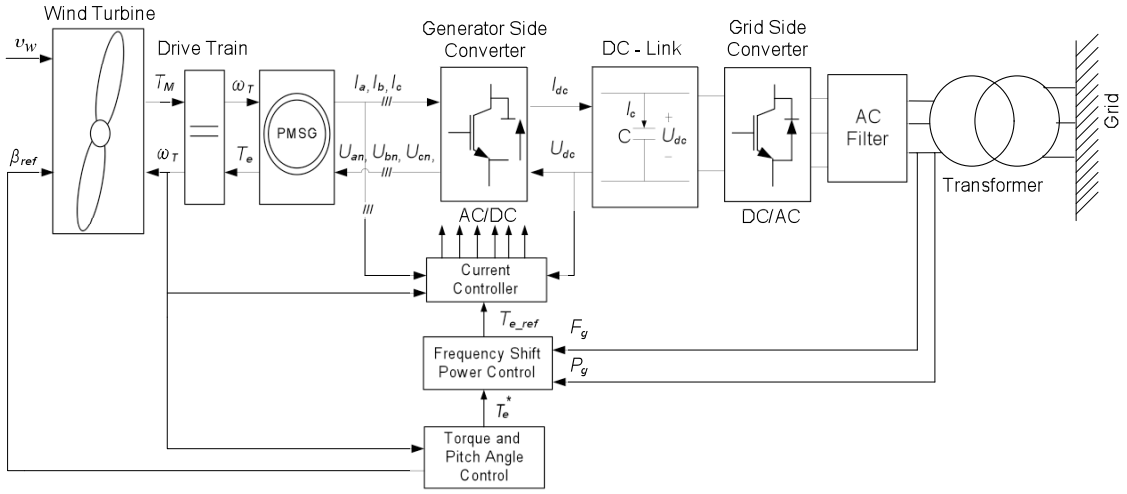

Figure 3.- PMSG driven wind turbine connected to the utility grid

Figure 3 shown a wind turbine system with its control scheme. Generator side controller is divided into a current controller, a frequency shift power control (FSPC) and Torque and Pitch Angle control. Theses controller will be briefly presented in section III. The input signals to the Generator side controller are: Grid Frequency (F_g), Grid Power (P_g), turbine rotor speed (ω_T), three phase sinusoidal current from PMSG (I_a, I_b, I_c) and the voltage of the dc bus capacitors (U_{dc}). The output signals are reference pitch angle (β_{ref}) and Generator Side Converter control

II. SYSTEM DESCRIPTION AND MODELING

The description and the modeling of a wind turbine with PMSG are described throughout this section. The mechanical components of the Wind Turbine System (the wind turbine rotor and the drive train) as well as the electrical components (the synchronous generator and the generator side converter) will be briefly presented.

A. Wind Turbine Model

The power in the wind is known to be proportional to the cube of the wind speed and may be expressed as

$$P = \frac{1}{2}\rho A v_w^3, \tag{1}$$

where ρ is the air density, A is the area swept by the blades and v_w is the wind speed. However, a wind turbine can only extract a fraction of the power, which is limited by the Betz limit (maximum 59%). This fraction is described by a power coefficient, C_p, which is a function of the blade pitch angle β and the tip speed ratio λ. Therefore the mechanical power of the wind turbine extracted from the wind by the turbine is

$$P_{mec} = \frac{1}{2}C_p(\beta,\lambda)\rho A v_w^3, \tag{2}$$

where the tip speed ratio λ is defined as the ratio between the blade tip speed and the wind speed v_w:

$$\lambda = \frac{\omega_T R}{v_w}, \tag{3}$$

ω_T is the turbine rotor speed and R is the radius of the blades. A hydraulic actuator model of pitch angle β control wind turbine is shown in Figure 4. The actuator is modeled in closed loop with saturation of the pitch rated limitation [6]. The maximum rate of change of the pitch angle is in the order of 3 to 10 degrees per second, depending on the size of the wind turbine. The signal β_{ref} is taken from *Torque and Pitch Angle Control*

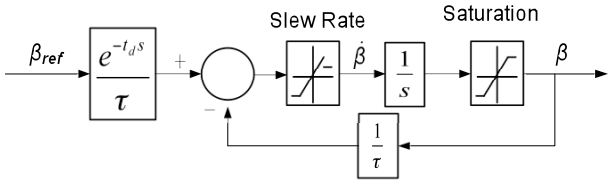

Figure 4.- Hydraulic Actuator Model

In this paper, the power coefficient is given by [7]

$$C_p(\lambda,\beta) = 0.5\left(\frac{114}{\lambda_i} - 0.4\beta - 3\right)\exp\left(\frac{-25}{\lambda_i}\right) + 0.000571\lambda, \tag{4}$$

Where

$$\lambda_i = \left[\frac{1}{\lambda + 0.08\beta} - \frac{0.035}{\beta^3 + 1}\right]^{-1} \tag{5}$$

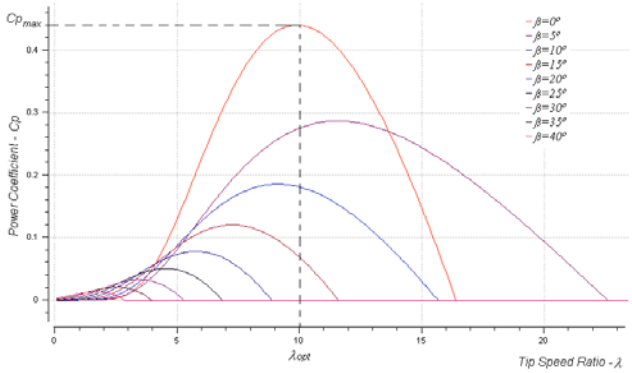

Figure 5.- Power coefficient versus tip-speed ratio

Thus, any changes in the rotor or wind speeds induce changes in the tip speed ratio, leading to power coefficient

variation. In this way, the generated power is affected. Figure 5 shows a typical C_P-λ curve for a wind turbine that follows (4). The wind turbine power coefficient is maximized (C_{p_max}=0.44) for a tip-speed ratio of λ_{opt}=6.9 when the blades pitch angle is β=0°.

The wind turbine is said to have a yaw error, if the rotor is not perpendicular to the wind. Considering θ_w as the wind direction and θ_t the yaw turbine angle, then the yaw error angle θ_c is defined as the difference between θ_w and θ_t.

$$\theta_c = \left| \theta_w - \theta_t \right| \tag{6}$$

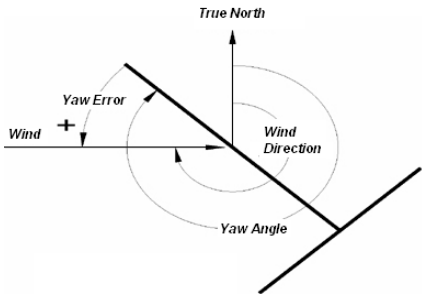

Figure 6.- Yaw angle convention

θ_c implies that a small wind energy share is going to be converted. The turbine generated power follows a cosine function of θ_c.

$$P_{mec} = P_{mec}(\theta_w)\cos(\theta_c) \tag{7}$$

B. Drive Train Model

The mechanical system of the wind turbine can be simply modeled with the one-mass model given by [8]:

$$J_{total}\frac{\partial \omega_T}{\partial t} = T_M - T_e, \tag{8}$$

where $J_{total}=J_T+J_g$ is the inertia constant of the whole drive train, with J_T and J_g the inertia constants of the turbine and the generator, respectively; n_p is the number of pole pairs; T_e is the generator electromagnetic torque and the mechanical torque of the turbine T_M is given by

$$T_M = \frac{P_{mec}}{\omega_T} = \frac{1}{2}\frac{C_p(\beta,\lambda)\rho A v_w^3}{\omega_T}, \tag{9}$$

C. Permanent Magnet Synchronous Generator Model

The rotor excitation of the Permanent Magnet Synchronous Generator (PMSG) is assumed to be constant, so its electrical model in the synchronous reference frame is given by [9, 10]:

$$L_S\frac{\partial i_{ds}}{\partial t} = u_{ds} - R_S i_{ds} + L_S\omega_e i_{qs}, \tag{10}$$

$$L_S\frac{\partial i_{qs}}{\partial t} = u_{qs} - R_S i_{qs} - L_S\omega_e i_{ds} + \omega_e\psi_f, \tag{11}$$

where subscripts'd' and 'q' refer to the physical quantities that have been transformed into the dq synchronous rotating reference frame; R_s is the stator resistance; L_s is the inductances of the stator; u_{ds} and u_{qs} are, respectively, the d- and q- axis components of stator voltage; i_{ds} and i_{qs} are, respectively, the d- and q- axis components of stator current; ψ_f is the permanent magnetic flux and the electrical rotating speed ω_e is given by:

$$\omega_e = n_p\omega_T, \tag{12}$$

Considering Inverse Park and Clarke Transformation a two co-ordinate time invariant (i_{qs}, i_{ds}) is transformed into a three phase sinusoidal system (I_a, I_b, I_c), where are the inputs to the generator side converter model.

$$\begin{bmatrix} I_a \\ I_b \\ I_c \end{bmatrix} = \begin{bmatrix} \cos(\omega_e t) & -\sin(\omega_e t) \\ \cos\left(\omega_e t - \frac{2\pi}{3}\right) & -\sin\left(\omega_e t - \frac{2\pi}{3}\right) \\ \cos\left(\omega_e t + \frac{2\pi}{3}\right) & -\sin\left(\omega_e t + \frac{2\pi}{3}\right) \end{bmatrix} \begin{bmatrix} i_{ds} \\ i_{qs} \end{bmatrix} \tag{13}$$

The power equations are given by

$$P_s = \frac{3}{2}\left(u_{ds}i_{ds} + u_{qs}i_{qs}\right), \tag{14}$$

$$Q_s = \frac{3}{2}\left(u_{qs}i_{ds} - u_{ds}i_{qs}\right), \tag{15}$$

where P_s and Q_s are the output active and reactive powers, respectively.

The electromagnetic torque T_e can be derived from

$$T_e = -\frac{3}{2}n_p\psi_f i_{qs}, \tag{16}$$

D. Generator Side Converter Model

Nowadays the back-to-back Voltage Source Converter (VSC) is the most used converter topology in the wind turbine industry as depicted in Figure 7. This converter can operate in rectifier or inverter mode, thus a bi-directional power flow can be achieved. In the present paper, the generator side converter works as a rectifier, being able to control the torque and speed, while the grid side converter works as an inverter keeping constant the voltage in the DC-link [11].

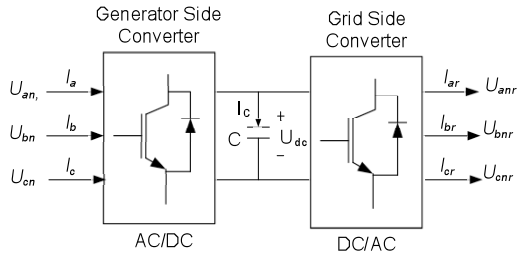

Figure 7.- Structure of the back-to-back voltage source converter

A VSC can be implemented in several ways: six-step, Pulse Amplitude Modulated (PAM) or Pulse Width Modulated (PWM). The paper is focused on the implementation of a PWM VSC, but the idea can be easily extended to other configurations.

A three-phase rectifier is shown in Figure 8: U_{dc} is the voltage of the dc bus capacitors; U_{an}, U_{bn} and U_{cn} are the phase voltage and each switch is identified with the letter S. It is assumed

that S_a and S_a^*, S_b and S_b^* as well as S_c and S_c^* are switched in a complementary way to avoid a short circuit in the voltage source. Thus, the analysis of the switches turn-ons/offs is simplified as we only consider the switches of the three upper transistors S_a, S_b and S_c. If S_a is equal to 1, the switch of the transistors is on and vice verse. As we have three variables, there are (2^3=8) possible switching vectors; as shown in Table I.

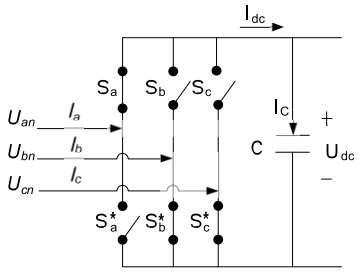

Figure 8.- Structure of the back-to-back voltage source converter

The applied voltages at the Permanent Magnet Synchronous Generator terminals as a function of the DC-link voltage and the switching functions are:

$$\begin{bmatrix} U_{an} \\ U_{bn} \\ U_{cn} \end{bmatrix} = \frac{U_{dc}}{3} \begin{bmatrix} 2 & -1 & -1 \\ -1 & 2 & -1 \\ -1 & -1 & 2 \end{bmatrix} \begin{bmatrix} S_a \\ S_b \\ S_c \end{bmatrix} \quad (17)$$

Considering Park and Clarke Transformation a three phase sinusoidal system (U_{an}, U_{bn}, U_{cn}) is transformed into a two co-ordinate time invariant (u_{ds} ,u_{qs}, u_o), where are the inputs to the Permanent Magnet Synchronous Generator (PMSG) Model. The angle used to make the transformation is given by:

$$\theta = \omega_e t \quad (18)$$

Considering this angle, the transformation gives:

$$\begin{bmatrix} u_{ds} \\ u_{qs} \\ u_o \end{bmatrix} = \frac{2}{3} \begin{bmatrix} \cos(\theta) & \cos\left(\theta - \frac{2\pi}{3}\right) & \cos\left(\theta + \frac{2\pi}{3}\right) \\ -\sin(\theta) & -\sin\left(\theta - \frac{2\pi}{3}\right) & -\sin\left(\theta + \frac{2\pi}{3}\right) \\ \frac{1}{2} & \frac{1}{2} & \frac{1}{2} \end{bmatrix} \begin{bmatrix} U_{an} \\ U_{bn} \\ U_{cn} \end{bmatrix} \quad (19)$$

The DC-link current can be expressed as a function of the input currents and the switching functions by:

$$I_{dc} = \begin{bmatrix} S_a & S_b & S_c \end{bmatrix} \begin{bmatrix} I_a \\ I_b \\ I_c \end{bmatrix} \quad (20)$$

III. MODEL OF CONTROLLERS

A. Current controller Model

The current control scheme of the generator side converter is show in Figure 9. This control is based on projections which transform a three phase time and speed dependent system into a two co-ordinate (d and q co-ordinates) time invariant system. These projections lead to a structure similar to that of a DC control that make easier AC control [12]. In order to design independent controllers for the two coordinates, the influences of the q-axis on the d-axis component, and vice versa, must be eliminated [13]. For this the decoupling voltages u_{ddec} and u_{qdec} are given by

$$u_{ddec} = u'_{ds} - L_s \omega_e i_{qs} \quad (21)$$

$$u_{qdec} = u'_{qs} + L_s \omega_e i_{ds} - \omega_e \psi_f \quad (22)$$

These decoupling voltages are added to the current controller outputs, resulting in the control signal for the PWM-rectifier. In order to combine a fast response of the controlled variable to a change of the set point with zero steady state deviation, proporcional integral (PI) current controllers are chosen. Control equations are given by:

$$\frac{\partial x_1}{\partial t} = i_{ds\_ef} - i_{ds} \quad (23)$$

$$\frac{\partial x_2}{\partial t} = i_{qs\_ef} - i_{qs} \quad (24)$$

$$u'_{ds} = K_{p1} \Delta i_{ds} + K_{i1} x_1 \quad (25)$$

$$u'_{qs} = K_{p2} \Delta i_{qs} + K_{i2} x_2 \quad (26)$$

The required d-q components of the rectifier voltage vector are given by:

$$u_{ds\_ref} = K_{p1} \Delta i_{ds} + K_{i1} x_1 - L_s \omega_e i_{qs} \quad (27)$$

$$u_{qs\_ref} = K_{p2} \Delta i_{qs} + K_{i2} x_2 + L_s \omega_e i_{ds} - \omega_e \psi_f \quad (28)$$

The control requires the measurement of the stator currents, dc voltage and rotor position. Space Vector Modulation (SVM) is used to generate the switching signals for the power converter semiconductors.

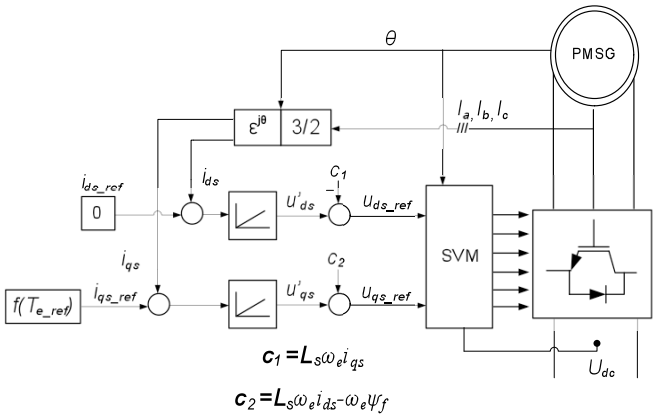

Figure 9.- Current controller Model

The stator current reference in d-axis $i_{ds\text{-}ref}$ is maintained at zero, for producing maximum torque, due to the non-saliency of the generator. The stator current reference in q-axis $i_{qs\text{-}ref}$ is calculated from the reference torque $T_{e\text{-}ref}$ as follows.

$$i_{qs\_ref} = -\left(\frac{2}{3 n_p \psi_f}\right) T_{e\_ref} \quad (29)$$

B. *Frequency Shift Power Control Model*

If Wind Turbine System (WTS) is connected to the AC side of the stand-alone hybrid system, as depicted in Figure 10, battery inverter must be able to inform to the WTS when it must limit its output power in order to prevent the excess energy from overcharging the battery. The communication language is frequency. In other words, the battery inverter recognizes this situation and changes the frequency at the AC output. This frequency is analyses by Wind Turbine System which limits its output power according to the frequency previously defined by battery inverter. The operating principle used by WTS is called Frequency Shift Power Control (FSPC) [14]. This function is shown in the Figure 11, for more information read Sunny Island 5048 Manual

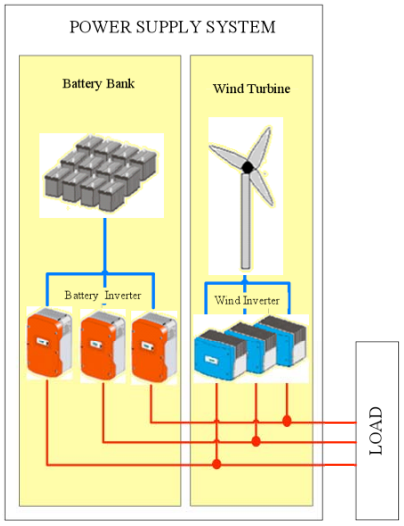

Figure 10.- Block diagram of a stand-alone grid

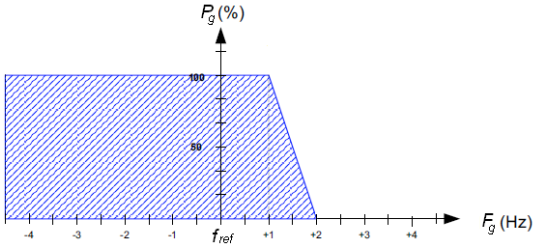

Figure 11.- Frequency Shift Power Control

f_{ref} refers to the base frequency of the stand- alone grid, in our case, it is equal to 50Hz. When the grid frequency deviation is less than 1 Hz and higher than -5Hz, $\%P_g$ is equal to 100%; when a grid frequency deviation occurs between 1 and 2 Hz, $\%P_g$ is different from 100% and when the grid frequency deviation is higher than 2 Hz, $\%P_g$ is equal to 0%.

The control scheme is depicted in Figure 12. When a grid frequency deviation Δf occurs a bias power set point, ΔP, is generated follows function shown in Figure 11. Then, the bias power set point is divided into the turbine rotor speed ω_T to obtain a bias electric torque set point, ΔT_e, which is added to the electric torque set point T_e^* from *Torque and Pitch Angle Control* to calculate a reference electric torque, $T_{e\text{-}ref}$, which is used to calculate $i_{qs\text{-}ref.}$ in *Current Controller*.

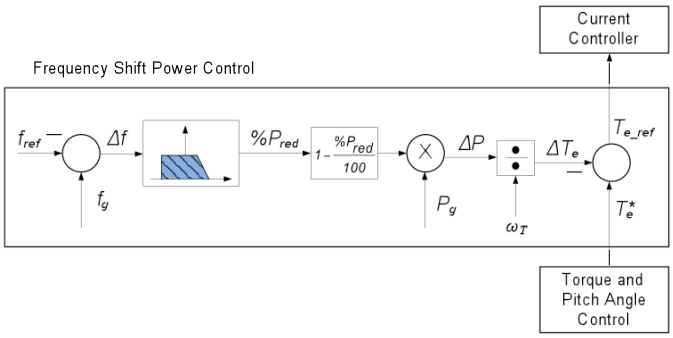

Figure 12.- Frequency Shift Power Control

C. *Torque and Pitch Angle Control*

From Figure 13, you can see that the power curve is split into three distinct regions. Region I consists of low wind speeds and is below the rated turbine power, the turbine is run at the maximum efficiency to extract all power. In other words, the turbine controls with optimization in mind. On the other hand, Region III consists of high wind speeds and is at the rated turbine power. The turbine then controls with limitation of the generated power in mind when operating in this region. Finally, Region II is a transition region mainly concerned with keeping rotor torque and noise low [15].

When the wind speed is lower than cut-in wind speed or higher than cut-out wind speed, the wind turbine could not generate power, and the pitch angle is usually set to 90°.

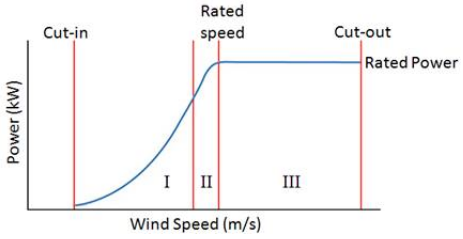

Figure 13.- Operating region of wind turbines

1.- Low Wind Speed Operation (Region I)

The main objective is to capture as much power as possible from the wind. All three control strategies (yaw drive, generator torque, and blade pitch) may be used in this region; however, it is common to use only generator torque and yaw control for most of the time in region 2, keeping the blade pitch constant at an optimal value β_{ref}=0°. To ensure maximal energy yield, the reference speed is set such that the tip speed ratio, λ is maintained at its optimal value, λ_{opt} according to equation X

$$\omega_T^* = \frac{\lambda_{opt}\, v_w}{R} \tag{30}$$

The control scheme is shown in Figure 14

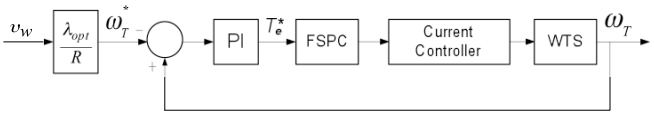

Figure 14.- Control scheme in low wind Speed

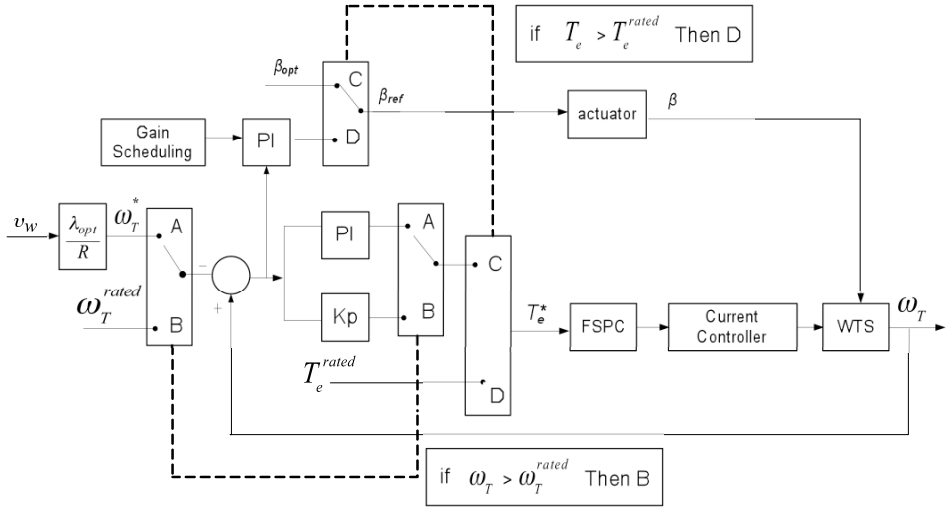

Figure 17.- Overview of the complete control scheme

2.- Middle Wind Speed Operation (Region II)

The main objective is to keep the rotor speed in a certain spam, described as a speed band around the maximum rotor speed. The rotor speed, torque and energy capture are determined similarly as in the case of a classic fixed speed wind turbine approach. Usually this interval ends when nominal generator power is reach so in this region turbine operate below rated power. The basic scheme is shown in Figure 15.

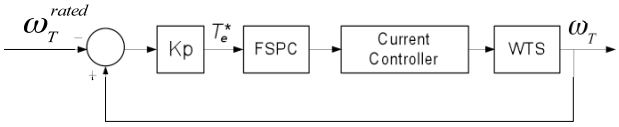

Figure 15.- Control scheme in middle wind Speed

3.- High Wind Speed Operation (Region III)

The main objective is to keep the rotor speed and especially the generated power as close as possible to the nominal. Yaw control, generator torque, and blade pitch strategies can all be used to shed excess power and limit the turbine's energy capture as well as to achieve other control objectives. The electric torque control objective is defined as production of constant rated electric power ($T_e^* = T_e^{rated}$), while the pitch control objective is defined as follows: Rotor speed regulation at rated rotor speed and yield of rated power, by controlling the blade pitch angle according to scheme shown in Figure 16.

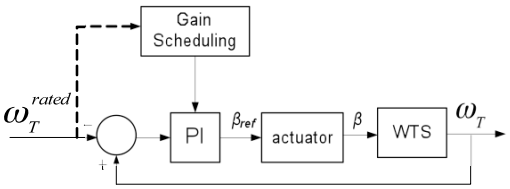

Figure 16.- Control scheme in high wind Speed

To cope with nonlinear turbine behavior caused by aerodynamics, the controller gains have been scheduled dependent on reference rotor speed. Adaptation of the rotor speed set point is a possibility that makes it possible to use the allowed rotor speed fluctuation for maintaining rated power at sudden negative wind gusts.

The control overview scheme is shown in Figure 17. It is not possible to operate in the whole speed area using only one controller and due to this the final controller is a combination of the controllers from the various wind speed intervals. Finally, after modelling and analyzing those three different controllers, the whole control scheme is obtained [16].

D. Yaw Mechanism

Horizontal axis wind turbines (HAWT) need extra devices to orientate their rotors against the wind. Yaw control would be an excellent way of controlling the power input to the wind turbine rotor. The main problem with yaw control is that the part of rotor which is closest to the source direction of the wind, however, will be subject to a large force (bending torque) than the rest of the rotor.

The yaw mechanism can be divided into two types: passive (free yaw) and active (forced yaw). Passive yaws have large application in small wind turbines. The turbine freely aligns itself to the wind direction by using a tail vane, with no need of wind measurement. Rotors with downwind configuration are another example of use of passive yaws.

IV. SPACE VECTOR MODULATION

Space Vector Modulation (SVM) became a standard for the switching power converters. The block diagram of (SVM) is shown in Figure 18. The reference output voltage vector is sampled at a fixed frequency, equal to the inverter switching period T_s. Then, the position of reference vector and the times of application of each vector generators involved are calculated. After that, a switching sequence system takes these application times to define the switches control signal. Thus, the reference vector will be really reflected in the output of the inverter during the switching period next to the reference voltage sampled time [17].

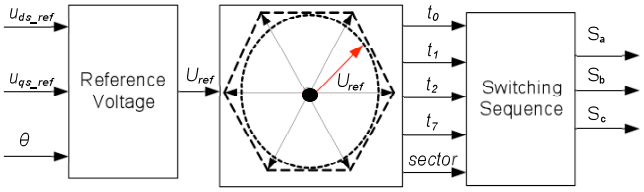

Figure 18.- Block diagram of Space Vector Modulation (SVM)

The reference voltage components in the dq reference frame ($u_{ds\text{-}ref}$, $u_{qs\text{-}ref}$) are transformed to a stationary $\alpha\beta$ reference frame using the rotor position θ as given by

$$\omega_T = \frac{\partial\theta}{\partial t}, \tag{31}$$

$$\begin{bmatrix} u_{\alpha ref} \\ u_{\beta ref} \end{bmatrix} = \begin{bmatrix} cos\theta & -sin\theta \\ sin\theta & cos\theta \end{bmatrix} \begin{bmatrix} u_{ds\_ref} \\ u_{qs\_ref} \end{bmatrix}, \tag{32}$$

where ($u_{\alpha ref}$, $u_{\beta ref}$) form an orthogonal 2-phase system. A rotating vector can be uniquely defined in the complex plane by these components as follows:

$$U_{ref} = u_{\alpha ref} + j\,u_{\beta ref} \tag{33}$$

The magnitude and angle of the output reference vector are

$$\left|U_{ref}\right| = \sqrt{u_{\alpha ref}^2 + u_{\beta ref}^2} \tag{34}$$

$$\varphi = Tan^{-1}\left(\frac{U_{\beta ref}}{U_{\alpha ref}}\right) \tag{35}$$

As shown in the Table I, the eight inverter states give eight vectors called *vector generators* (**U0, U1, ..., U7**), which are divided into 6 active switching vectors **U1, U2, ..., U6** plus 2 vectors corresponding to the zero states **U0** and **U7,** where the magnitude of the active vectors is $(2/3)U_{dc}$. Since the output voltages are at $2\pi/3$ out of phase from each other, the Space Vectors system can occupy a number of positions with an order multiple of three.

The vector generators on the αβ plane are shown in Figure 19. The tips of these vectors form a regular hexagon. We define the area enclosed by two adjacent vectors, within the hexagon, as a *sector*. Thus there are six sectors numbered 1 to 6 [18].

The reference vector, U_{ref}, placed on the αβ plane, is decomposed using any subset of the eight space vectors. Nonetheless, decomposition is done typically using only the two adjacent active vectors, by averaging the two adjacent vectors and the zero state vectors. In other words, the switching pattern is obtained by selecting the nearest two active vectors of the six available and filling the rest of the switching period with zero space vectors **U0** and **U7**.

Voltage Vector	S_a	S_b	S_c
U0 = 0	0	0	0
U1 = $\left(\frac{2}{3}\right)U_{dc}$	1	0	0
U2 = $\left(\frac{1}{3}\right)U_{dc} + j\left(\frac{\sqrt{3}}{3}\right)U_{dc}$	1	1	0
U3 = $-\left(\frac{1}{3}\right)U_{dc} + j\left(\frac{\sqrt{3}}{3}\right)U_{dc}$	0	1	0
U4 = $-\left(\frac{2}{3}\right)U_{dc}$	0	1	1
U5 = $-\left(\frac{1}{3}\right)U_{dc} - j\left(\frac{\sqrt{3}}{3}\right)U_{dc}$	0	0	1
U6 = $\left(\frac{1}{3}\right)U_{dc} - j\left(\frac{\sqrt{3}}{3}\right)U_{dc}$	1	0	1
U7 = 0	1	1	1

Table I.- Inverter Voltage Vectors

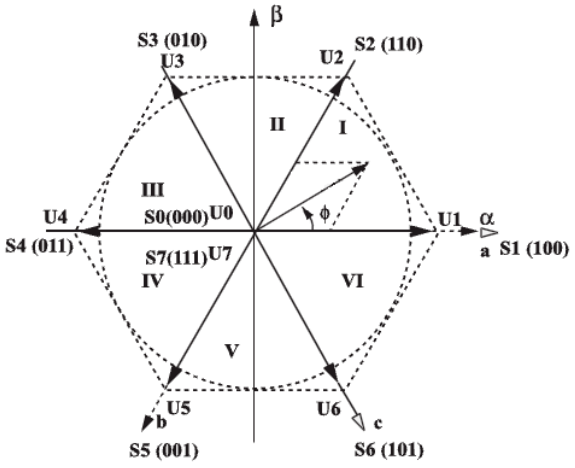

Figure 19.- Voltage space vectors on the αβ plane

In the particular example of Figure 20, the reference vector is represented by an vector U_{ref} rotating in the counter

clock wise direction, located between 0° and 60° degree, the two adjacent active vectors are **U1** and **U2**.

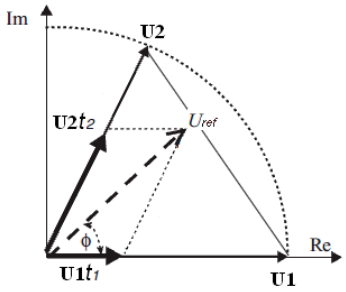

Figure 20.- Reference Vector placed on the αβ plane

The time spent on each of the active space vectors (denoted t_0, t_1, t_2 and t_7) are determinated by

$$U_{ref} = \frac{t_1}{T_s}\mathbf{U1} + \frac{t_2}{T_s}\mathbf{U2} + \frac{t_0}{T_s}\mathbf{U0} + \frac{t_7}{T_s}\mathbf{U7}, \quad (36)$$

Considering that the magnitudes of zero space vectors **U0** and **U7** are 0, we obtain

$$T_s U_{ref} = \mathbf{U1}t_1 + \mathbf{U2}t_2, \quad (37)$$

where T_s is the switching period; t_1 and t_2 are the time spent respectively on the two active vectors **U1** and **U2** adjacent to the reference vector. Decomposition along the Real and Imag axes yields

$$T_s\left|U_{ref}\right|\cos\varphi = \frac{2}{3}U_{dc}t_1 + \frac{1}{3}U_{dc}t_2 \quad (38)$$

$$T_s\left|U_{ref}\right|\sin\varphi = 0t_1 + \frac{\sqrt{3}}{3}U_{dc}t_2 \quad (39)$$

with the solution:

$$t_1 = \frac{3\left|U_{ref}\right|T_s}{2U_{dc}}\left[\cos\varphi - \frac{\sin\varphi}{\sqrt{3}}\right] = \frac{\sqrt{3}\left|U_{ref}\right|}{U_{dc}}T_s\sin\left(\frac{\pi}{3} - \varphi\right) \quad (40)$$

$$t_2 = \frac{\sqrt{3}\left|U_{ref}\right|}{U_{dc}}T_s\sin\varphi \quad (41)$$

Zero state vectors are used to fill-up the gap to a constant sampling interval. t_0 and t_7 is the time spent on the zero space vectors **U0** and **U7**, respectively.

$$t_0 + t_7 = \frac{T_s - t_1 - t_2}{2} \quad (42)$$

The angle of reference vector, φ, identifies one of the six sectors on αβ plane. An relative angle, ε_r ($0 \le \varepsilon_r \le \pi/3$), is defined according to a specific sector, such as

$$\varepsilon_r = \varphi - (r-1)\frac{\pi}{3}, \qquad r = 1,2,\ldots,6 \quad (43)$$

The application times are given by

$$t_a = \frac{\sqrt{3}\left|U_{ref}\right|}{U_{dc}}T_s\sin\left(\frac{\pi}{3} - \varepsilon_r\right) \quad (44)$$

$$t_b = \frac{\sqrt{3}\left|U_{ref}\right|}{U_{dc}}T_s\sin\varepsilon_r \quad (45)$$

Switching Sequence Schemes

The active space vectors generate the same average output voltage regardless of the order in which they are applied within the current sampling period. SVM does not recommend any specific order. These degrees of freedom make the difference between Space Vector methods.

Space vector modulation also offers flexibility with zero vectors. They can be used in any order within the switching period and relative to active vectors. The order of individual zero vectors during the inactive time is another degree of freedom.

In this paper we have chosen the switching sequence called Symmetric Sequence: each switching period starts and ends with a zero vector and active vectors are exchanged. The reference voltage can be constructed by the switching pattern shown in Figure 21. **Ux** can be **U1**, **U3**, **U5**. **Uy** can be **U2**, **U4**, **U6**. This pattern satisfies the condition that only one transistor is switched during a change interval. This scheme is expected to have low THD (***T**otal* ***H**armonic* ***D**istortion*) because of the symmetry in the waveforms [19].

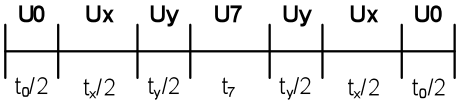

Figure 21.- Switching pattern for Symmetric Sequence

The switching pattern for different sectors is shown in the Figure 22.

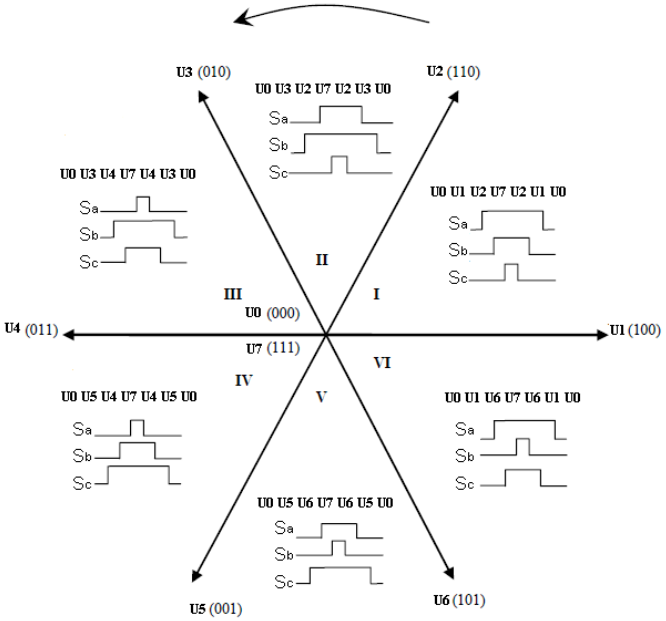

Figure 22.- Switching pattern for different sectors

In the example of Figure 23, the sequence of vectors applied in this scheme is shown in Figure 11 for sector 1. The number of commutations in one switching period is six with three turn-ons and three turn-offs.

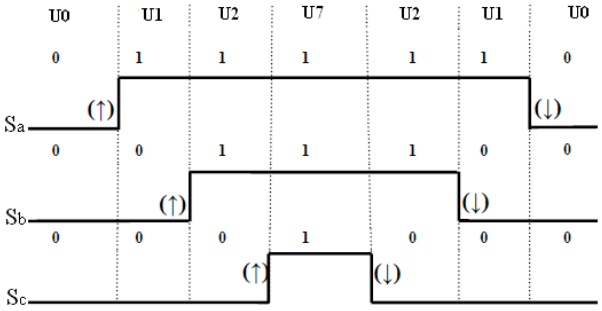

Figure 23.- Switching pattern for vector reference located in the sector 1

V. CONCLUSION

This work has presented the modelling of a wind turbine system equipped with a Permanent Magnet Synchronous Generator (PMSG) for dynamical simulation and controller design. PMSG generated voltage is converted into DC voltage though a Voltage Source Converter (VSC) that works as rectifier. The generator side converter is used to control power; the grid side converter is used to control dc-link voltage. The DC-link capacitor voltage is maintained at a constant value by ensuring the balance of the input and output energies at both sides of the capacitor. The future work will be to complete the scheme wind turbine system, simulate the whole system and compare this result with typical configurations for controller design.

REFERENCE

[1] H. Polinder, F. F. A. Van De Pijil, G. J. De Vilder and P. J. Tavner, "*Comparison of direct drive and geared generator concepts for wind turbine*", IEEE Trans. Energy Conver. 21(3) (2006) 725-733

[2] J.G. Slootweg, S.W.H. de Haan, H. Polinder, and W.L. Kling, "*Modeling wind turbines in power system dynamics simulations"* IEEE Power Engineering Society Summer Meeting, vol. 1, July 2001,pp. 22 – 26.

[3] Fujin Deng and Zhe Chen, "*Power Control of Permanent Magnet Generator Based Variable Speed Wind Turbines"*, IEEE Trans Energy Conver. (2006).

[4] J. Salazar, F. Tadeo, C. Prada. "*Renewable Energy for Desalinization using Reverse Osmosis*" International Conference on Renewable Energies and Power Quality (ICREPQ'10) Granada (Spain), 23th to 25th March, 2010

[5] DENG Qiu-ling, LIU Gou-rong and XIAO Feng. "*Control of Variable-speed Permanent Magnet Synchronous Generators Wind Generation System*". IEEE Trans Energy Conver (2008).

[6] Fernando D. Bianchi, Hernan De Battista, and Ricardo J. Mantz. "*Wind Turbine Control Systems*". British Library Cataloguing, 2007.

[7] Raiambal K. y Chellamuthu C. "*Modelling and simulation of grid connected wind electric generating system*". Anales de IEEE TENCON, 1847-1852. 2002

[8] F. Mei, B. C. Pal, "*Modelling and small-signal analysis of a grid connected doubly-fed induction generator*" presented at Proceeding of IEEE PES General Meeting 2005, San Francisco, USA, 2005.

[9] F. Wua, X.-P. Zhangb, P. Jua; "*Small signal stability analysis and control of the wind turbine with the direct-drive permanent magnet generator integrated to the grid*"; 2009

[10] Dmitry Svechkarenko, "*Simulations and Control of Direct Driven Permanent Magnet Synchronous Generator*", Proyect Work, Royal Institute of Technology, Department of Electrical Engineering, Electrical Machines and Power Electronics, December, 2005.

[11] Cristian Busca, Ana-Irina Stan, Tiberiu Stanciu and Daniel Ioan Stroe. "*Control of Permanent Magnet Synchronous Generator for Large Wind Turbines*". IEEE (2008).

[12]. A.J. Mahdi, W.H. Tang, L. Jiang and Q.H. Wu. "*A Comparative Study on Variable-Speed Operations of a Wind Generation System Using Vector Control*". International Conference on Renewable Energy (ICREPQ'10). (Granada, Spain). 23rd to 25th March, 2010.

[13] Mónica Chinchilla, Santiago Arnaltes and Juan Carlos Burgos; "*Control of Permanent-Magnet Generators Applied to Variable-Speed Wind-Energy Systems Connected to the Grid*"; March 2006

[14] *Sunny island 5048, Installation and Instruction Manual.* www.sma.de/en/products/off-grid-inverters/sunny-island-5048-5048u.html. Last View: June 28, 2010

[15] Mika Rasila. "*Torque- and Speed Control of a Pitch Regulated Wind Turbine*". Department of Electric Power Engineering Chalmers University of Technology. Goteborg, Sweden 2003

[16] Arkadiusz Kulka. "*Pitch and Torque Control of Variable Speed Wind Turbines*". Department of Electric Power Engineering. Chalmers University of Technology. Goteborg, Sweden 2004.

[17] YANG Yong, RUAN Yi, SHEN Huan-qing, TANG Yan-yan and YANG Ying. "*Grid-connected inverter for wind power generation system*" J Shanghai Univ (Engl Ed), 2009, 13(1): 51–56

[18] D.C. Aliprantis S.A. Papathanassiou M.P. Papadopoulos A.G. Kladas; "*Modeling and control of a variable-speed wind turbine equipped with permanent magnet synchronous generator*"; March 2008

[19] V.Himamshu Prasad, Dushan Boroyevich and Richard Zhang; "*Analysis and Comparison of Space Vector Modulation Schemes for a Four-Leg Voltage Source Inverter*"; 2006